Final-state interaction in inclusive electromagnetic nuclear processes

Y. Horikawa,* F. Lenz, and Nimai C. Mukhopadhyay
Swiss Institute for Nuclear Research (SIN), 5234 Villigen, Switzerland
(Received 20 March 1980)

The problem of nucleon final-state interaction in inclusive electromagnetic reactions is discussed within an optical potential description for the outgoing nucleon. The formalism accounts for both the loss of flux in the primary one-nucleon removal channel and the excitation of the multinucleon ones. Thereby a crucial difficulty encountered in the distorted-wave Born-approximation treatments of inclusive processes is eliminated. The calculation has been applied to the (e,e') reaction at the Stanford kinematics of 500 MeV incident energy and 60° scattering angle. As a result of nucleon final-state interaction, the peak intensities are reduced by 5–10 %; about half of the (e,e') reaction is found to correspond to multinucleon removal. In contrast to the good agreement of the calculation with the Stanford data, severe discrepancies are obtained if applied to the recent Saclay data for incident energies around 400 MeV. The limitations of our approach are explored by considering processes at relatively low momentum transfers: low-energy electron scattering and radiative pion capture.

[NUCLEAR REACTIONS Inclusive electron scattering. Radiative pion capture. Green's function approach. DWBA. Targets $4 \leq A \leq 58$. Electron energy 100–500 MeV, $\theta = 60°$; stopped pion.]

I. INTRODUCTION

At high energies exclusive nuclear reactions such as elastic scattering or excitation of discrete states, are described with great success by theories which are based, in one form or the other, on the multiple scattering formalism. We particularly emphasize the success of the optical potential approach to elastic scattering and of the related distorted-wave impulse approximation (DWIA) in the description of nuclear excitations. The reason for this success is that, at high energies, the projectile-nucleus interaction is dominated by "quasifree" nucleon knockout, in agreement with the basic assumptions of the multiple scattering concept. This dominance of knockout processes makes rearrangement processes or coupled channel effects unimportant, and thereby leads to a rather simple picture of the scattering process, compared to low-energy scattering.

In contrast to exclusive reactions, these high-energy concepts have not been systematically applied to the study of inclusive reactions. Although one can start from the dominance of nucleon knockout, it is clear that the techniques for describing these reactions must be different if the final state remains unspecified. In the exclusive reactions, nucleon knockout in the initial and final states leads to an attenuation of the flux in the channel considered. This is described by the imaginary part of the optical potential. In an inclusive reaction, however, these multistep processes contribute to the observed reaction as well and, therefore, cannot be taken into account by simply distorting, and thereby attenuating, the incoming and outgoing waves. For a strongly interacting projectile, the situation is rather complicated, since both the projectile and the knocked-out nucleon may further interact with the residual nucleus, giving rise to multistep processes with excitation of complicated structures. In this work, we study the problem of final-state interaction in the simpler case of the (e,e') reaction, where only the knocked-out nucleon interacts with the residual nucleus.

For the exclusive $(e,e'p)$ reaction, one accounts for the proton final-state interaction by generating the outgoing proton wave in the complex optical potential.[1,2] However, for inclusive reaction, a real potential (possibly momentum and/or energy dependent) is usually employed in generating the outgoing proton wave.[3-5] From the theoretical point of view, this is very unsatisfactory, since, at finite energies, the single-particle potential has to be complex due to the presence of open channels.

In this paper, we shall show that the same theoretical concept applies to both the exclusive $(e,e'p)$ and the inclusive (e,e') reaction. In Sec. II we develop these concepts. In Sec. III, these theoretical considerations will be applied to the Stanford 500 MeV (e,e') data.[6] For these kinematics, one can expect the high-energy approximations involved, such as identification of the optical potential in the ground and excited states of the nucleus, respectively, and neglect of correlations,

to be valid. In the actual calculation, we do not use the high-energy approximation to the optical potential, but rather a phenomenological optical potential. In this way, we are able to discuss the influence of this specific type of final-state interaction at comparatively low excitation energies as well. In Sec. IV, we show the limitation of the approach when applied to the inclusive (e,e') reaction with electron incident energy around 100 MeV,[7] and radiative π capture,[8] where the dominant contribution is no longer quasifree and where particle-hole rescattering and ground-state correlations become important. We summarize our conclusions in Sec. V.

II. FINAL-STATE INTERACTION IN EXCLUSIVE AND INCLUSIVE (e,e') REACTIONS

We start our discussion by considering the exclusive $(e,e'N)$ reaction on a nucleus. The differential cross section is given by

$$\frac{d^3\sigma}{d\Omega\, d\omega\, d\vec{p}_f} = K\,\delta(\omega-(E_f-E_0)) \times \left|\left\langle \vec{k}_f, \psi^{A-1}_{\vec{p}_f}\right| \sum_{i=1}^{A} \hat{t}_i \left|\vec{k}_i, 0\right\rangle\right|^2 , \tag{1}$$

where $\hat{t}_i$ is the elementary e-N t matrix, and K is a kinematic factor depending only on the energies of the incoming and outgoing electron; ω is the energy loss of an electron scattered into solid angle Ω, $\vec{k}_i$ and $\vec{k}_f$ are momenta of the incoming and ougoing electron. $|0\rangle$ is the nuclear ground state, $|\psi_{\vec{p}_f}\rangle$ an excited state of the nucleus of energy E_f and with a proton of asymptotic momentum $\vec{p}_f$ in the continuum. In the evaluation of (1) for the $(e,e'p)$ reaction, one normally factorizes out the electron-nucleon cross section σ_{eN} (Ref. 9):

$$\frac{d^3\sigma}{d\Omega\, d\omega\, d\vec{p}_f} = \frac{m}{E_{p_f}}\sigma_{ep}\left|\left\langle \psi^{(-)}_{\vec{p}_f}\right| \sum_{i=1}^{Z} e^{i\vec{q}\cdot\vec{x}_i}\left|0\right\rangle\right|^2 \delta(\omega - E_f + E_0) , \tag{2}$$

where m is the nucleon mass; σ_{eN} is given, neglecting off-shell effects, in terms of the Mott cross section σ_M and the electric and magnetic form factors G_E and G_M of the nucleon:

$$\sigma_{eN} = \sigma_M\left[\left(1+\frac{|q_\mu{}^2|}{4m^2}\right)^{-1}\left(G_E{}^2+\frac{|q_\mu{}^2|}{4m^2}G_M{}^2\right) + 2\tan^2\frac{\theta}{2}\,\frac{|q_\mu{}^2|}{4m^2}G_M{}^2\right] \tag{3}$$

$$\equiv \sigma_M\left[T_2(q_\mu{}^2)+2\tan^2\frac{\theta}{2}T_1(q_\mu{}^2)\right], \tag{4}$$

where θ is the electron scattering angle, $q_\mu{}^2$ being the square of the four-momentum transfer. In the single-particle approximation to the nuclear matrix element in (2), the $(e,e'p)$ exclusive cross section is given by

$$\frac{d^3\sigma}{d\Omega\, d\omega\, d\vec{p}_f} = \sigma_{ep}\sum_h \left|\langle \phi^{(-)}_{\vec{p}_f}\left| e^{i\vec{q}\cdot\vec{x}}\right|\phi_h\rangle\right|^2 \times \delta\left(\omega-\epsilon_f+\epsilon_h-\frac{q^2}{2M_A}\right), \tag{5}$$

where the sum is over the occupied single-particle orbits of the (nuclear-ground-state) shell-model potential and $\phi_{\vec{p}_f}$ is the single-particle wave function of the knocked-out nucleon generated in the optical potential. ϵ_f and ϵ_h are the corresponding particle and hole energies, respectively. In contrast to the shell-model potential, the single-particle potential of the knocked-out nucleon contains an imaginary part. This imaginary part accounts for the attenuation in the final channel due to final-state interaction of the knocked-out nucleon with the residual nucleus. The resulting reduction of the exclusive $(e,e'p)$ cross section is important in the analysis of the experimental data (cf. Ref. 2).

The inclusive (e,e') cross section can be obtained by summing over all the final states compatible with energy conservation. The resulting formula can be written in terms of two structure functions $W_1(\omega,q_\mu{}^2)$ and $W_2(\omega,q_\mu{}^2)$:

$$\frac{d^2\sigma}{d\Omega\, d\omega} = \sigma_M[W_2(\omega,q_\mu{}^2)+2\tan^2(\theta/2)W_1(\omega,q_\mu{}^2)] . \tag{6a}$$

The structure functions are related to F_c and F_t, the squares of the nuclear charge and transverse form factors in the laboratory frame, by

$$W_1 = \tfrac{1}{2}F_t , \tag{6b}$$

$$W_2 = \frac{q_\mu{}^4}{q^4}F_c + \frac{q_\mu{}^2}{2q^2}F_t . \tag{6c}$$

In the nonrelativistic impulse approximation to F_c, the spin-dependent term vanishes up to the order (q^2/m^2) if we neglect the spin-orbit coupling. Therefore, F_c is given by the Coulomb response function

$$R_{p(n)}(\omega,q) = \sum_f \left|\left\langle f\right| \sum_{j=1}^{Z(N)} e^{i\vec{q}\cdot\vec{x}_j}\left|0\right\rangle\right|^2 \delta(\omega-(E_f-E_0)) = \frac{\mathrm{disc}}{2\pi i}\left\langle 0\right| \sum_j e^{-i\vec{q}\cdot\vec{x}_j}\frac{1}{\omega-H}\sum_k e^{i\vec{q}\cdot\vec{x}_k}\left|0\right\rangle . \tag{7}$$

We now discuss the evaluation of the response function. The single-particle approximation to the wave functions in (7) leads to the DWIA:

$$R_p(\omega,q) = \sum_{i=1}^{Z}\sum_f \langle \phi^{(-)}_{\vec{p}_f}(i)\left| e^{i\vec{q}\cdot\vec{x}_i}\right|\phi_i(i)\rangle\Big|^2 \times \delta\left(\omega+\epsilon_i-\epsilon_f-\frac{q^2}{2M_A}\right) . \tag{8}$$

This approximation to the response function has been used in several calculations for the inclusive (e,e') reaction.[3-5] From the theoretical point of view, this approximation is very problematic, since the single-particle potential at positive nucleon energies is necessarily complex due to the presence of open channels. As in the case of the exclusive $(e,e'p)$ reaction, an imaginary part in the single-particle potential leads to a loss of flux in the one-nucleon channel (1p-1h channel). In a large nucleus, the intensity of the outgoing nucleon wave function is strongly damped in the interior and, therefore, only nucleons in the surface contribute to the cross section. Thus, only $Z^{2/3}$ protons contribute to the quasielastic reaction instead of all the protons, i.e., this single-particle approximation violates the nonenergy weighted sum rule. To avoid this serious difficulty, the calculations mentioned above[3-5] simply use a phenomenological real potential. Although this procedure yields at least qualitative agreement with experiment, the theoretical problem remains as to why to use in the exclusive reaction a complex potential, but to disregard its imaginary part in the inclusive ones. To trace the origin of this problem, we treat this final-state interaction perturbatively, and apply the high-energy approximation to the optical potential.

In the high-energy approximation, the matrix element in (8) reads

$$\begin{aligned} M_i &= \langle \phi_{\vec{p}_f}^{(-)}(i) \,|\, e^{i\vec{q}\cdot\vec{x}_i} \,|\, \phi_i(i)\rangle = \langle \vec{p}_f \,|\, e^{i\vec{q}\cdot\vec{x}_i} \,|\, \phi_i(i)\rangle \\ &\quad + \langle \vec{p}_f \,|\, u(i) G_0(i) e^{i\vec{q}\cdot\vec{x}_i} \,|\, \phi_i(i)\rangle + \cdots \\ &= M_i^0 + M_i^1 + \cdots \end{aligned} \tag{9a}$$

with $G_0 = 1/(\omega - T + i\epsilon)$. In the single scattering approximation to $u(i)$, we have

$$u(i) = \sum_{j\neq i} \langle \phi_j(j) \,|\, t_{ij}(\omega) \,|\, \phi_j(j)\rangle , \tag{9b}$$

where $t_{ij}(\omega)$ is the N-N t matrix. Diagrammatically, Eq. (9a) is represented by

$M_i =$ 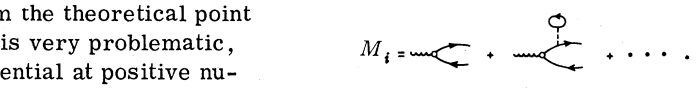 (9c)

The final-state interaction process (second diagram) reduces the plane wave impulse approximation result because of the imaginary part of u, i.e., due to the imaginary part of the N-N t matrix. Since the latter arises from the intermediate on-shell N-N states in the N-N interaction, the reduction of the 1p-1h excitation cross section is due to the true (on-shell) excitation of the 2p-2h states. Thus, if we want to include the final state interaction in the 1p-1h channel, we have to account for the true 2p-2h excitations simultaneously. In the perturbative approach, this requires an incoherent addition of the following matrix element to M_i:

$$M_{ij} = \langle \vec{p}_i \vec{p}_j \,|\, t_{ij} G_0(i) e^{i\vec{q}\cdot\vec{x}_i} \,|\, \phi_i(i)\phi_j(j)\rangle , \tag{10a}$$

$M_{ij} =$ 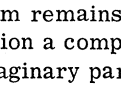 (10b)

In this approximation to the final-state interaction, the cross section is given by

$$\begin{aligned} \left(\frac{d^2\sigma}{d\Omega d\omega}\right)_i &\approx \int d^3p_f \,|M_i^0|^2 \delta\left(\omega - \frac{p_f^2}{2m}\right) \\ &\quad + 2\,\mathrm{Re}\int d^3p_f M_i^0 M_i^{1*} \delta\left(\omega - \frac{p_f^2}{2m}\right) \\ &\quad + \sum_j \int d^3p_i \, d^3p_j \,|M_{ij}|^2 \delta\left(\omega - \frac{p_i^2}{2m} - \frac{p_j^2}{2m}\right) \\ &= \left(\frac{d^2\sigma}{d\Omega d\omega}\right)_i^0 + \left(\frac{d^2\sigma}{d\Omega d\omega}\right)_i^1 . \end{aligned} \tag{11}$$

We now evaluate the correction $(d^2\sigma/d\Omega d\omega)_i^1$ due to final-state interaction and find, using $\delta(\omega - p_f^2/2m) = (2i\pi)^{-1}(G_0^\dagger - G_0)$,

$$2\,\mathrm{Re}\int d^3p_f M_i^{0*} M_i^1 \delta\left(\omega - \frac{p_f^2}{2m}\right) = \frac{1}{2i\pi}\langle \phi_i \,|\, e^{-i\vec{q}\cdot\vec{x}_i} [G_0^\dagger u^\dagger(i)(G_0^\dagger - G_0) + (G_0^\dagger - G_0) u(i) G_0] e^{i\vec{q}\cdot\vec{x}_i} \,|\, \phi_i\rangle , \tag{12a}$$

$$\begin{aligned} &\sum_j \int d^3p_i \, d^3p_j \,|M_{ij}|^2 \delta\left(\omega - \frac{p_i^2}{2m} - \frac{p_j^2}{2m}\right) \\ &\quad = \frac{1}{2i\pi} \sum_j \left\langle \phi_i(i)\phi_j(j) \left| e^{-i\vec{q}\cdot\vec{x}_i} G_0^\dagger t_{ij}^\dagger \left(\frac{1}{\omega - T_i - T_j - i\epsilon} - \frac{1}{\omega - T_i - T_j + i\epsilon}\right) t_{ij} G_0 e^{i\vec{q}\cdot\vec{x}_i} \right| \phi_i \right\rangle \\ &\quad = \frac{1}{2i\pi}\langle \phi_i(i) \,|\, e^{-i\vec{q}\cdot\vec{x}_i} G_0^\dagger [u^\dagger(i) - u(i)] G_0 e^{i\vec{q}\cdot\vec{x}_i} \,|\, \phi_i(i)\rangle , \end{aligned} \tag{12b}$$

where we have used in the last step the unitarity relation for the N-N t matrix:

$$t_{ij}^\dagger - t_{ij} = t_{ij}^\dagger \left(\frac{1}{\omega - T_i - T_j - i\epsilon} - \frac{1}{\omega - T_i - T_j + i\epsilon}\right) t_{ij} . \tag{12c}$$

Combining (12a) and (12b) we finally have for $(d^2\sigma/d\Omega d\omega)_i^1$

$$\left(\frac{d^2\sigma}{d\Omega d\omega}\right)_i^1 = \frac{1}{2i\pi}\langle \phi_i \,|\, e^{-i\vec{q}\cdot\vec{x}_i} [G_0^\dagger u^\dagger(i) G_0^\dagger - G_0 u(i) G_0] e^{i\vec{q}\cdot\vec{x}_i} \,|\, \phi_i\rangle . \tag{12d}$$

It is now straightforward to show that the modi-

fication of the cross section due to the final-state interaction does not change the sum rule. We have

$$\int_0^\infty \left(\frac{d^2\sigma}{d\Omega d\omega}\right)_i^1 = -\frac{1}{2i\pi}\int_c \langle\phi_i|e^{-i\vec{q}\cdot\vec{x}_i}G_0 u(i) G_0 e^{i\vec{q}\cdot\vec{x}_i}|\phi_i\rangle\,, \tag{13}$$

where the contour of integration is along the two rims of the unitary cut along the real axis. This contour can be deformed to infinity, which gives no contribution to the integral. Apart from possible bound state contributions of t_{ij}, corresponding to the $(e,e'd)$ reaction, the final-state interaction effects do not change the sum rule.

We can now generalize the above result by avoiding the perturbative treatment of the final-state interaction. We replace the diagrams in (9c) and (10b) by

$\bar{M}_i =$, (14a)

$\bar{M}_{ij} =$, (14b)

where the double bar represents the effect of the distortion; i.e., the final state in (14a) is written as

$$\langle\phi_{\vec{p}_f}^{(-)}(i)| = \langle\vec{p}_f|\Omega(i)\,, \tag{14c}$$

and the Green's function in (14b)

$$G(i) = G_0(i)\Omega(i)\,, \tag{14d}$$

with the Møller operator

$$\Omega(i) = 1 + u(i)G(i)\,. \tag{14e}$$

We now repeat, with these definitions, the calculations (11) and (12), and find immediately

$$\begin{aligned}
\overline{d\sigma}_i &= \int d^3p_f |\bar{M}_i|^2 \delta\left(\omega - \frac{p_f^2}{2m}\right) + \sum_j \int d^3p_i\, d^3p_f |M_{ij}|^2 \delta\left(\omega - \frac{p_i^2}{2m} - \frac{p_f^2}{2m}\right) \\
&= \frac{1}{2i\pi}\{\langle\phi_i|e^{-i\vec{q}\cdot\vec{x}_i}\Omega^\dagger(i)[G_0^\dagger(i) - G_0(i)]\Omega(i)e^{i\vec{q}\cdot\vec{x}_i}|\phi_i\rangle + \langle\phi_i|e^{-i\vec{q}\cdot\vec{x}_i}G^\dagger(i)[u^\dagger(i) - u(i)]G(i)e^{i\vec{q}\cdot\vec{x}_i}|\phi_i\rangle\} \\
&= \frac{1}{2i\pi}\langle\phi_i|e^{-i\vec{q}\cdot\vec{x}_i}[G^\dagger(i) - G(i)]e^{i\vec{q}\cdot\vec{x}_i}|\phi_i\rangle \\
&= -\frac{1}{2i\pi}\mathrm{disc}\langle\phi_i|e^{-i\vec{q}\cdot\vec{x}_i}G(i)e^{i\vec{q}\cdot\vec{x}_i}|\phi_i\rangle\,,
\end{aligned} \tag{15}$$

where we have used the definitions (14d) and (14e) to combine in (15) the contributions from the 1p-1h and the 2p-2h channels. Equation (15) is more general than our deviation, using explicitly the high-energy approximation, indicates. Equation (15) can be derived directly from Eq. (7) by writing the response function as the discontinuity of the many-body Green's function, and then approximating the latter by a single-particle optical Green's function. We have chosen the above procedure to display the common basis in the theories of exclusive and inclusive reactions. In this high-energy approximation, the final-state interaction effects in both the exclusive and inclusive reactions are determined by the same optical potential. In the exclusive $(e,e'p)$ reaction, the experiment selects the process (14a) only, and, therefore, the effect of the imaginary part of the optical potential is to attenuate the intensity of the outgoing proton wave. This loss of flux out of the one-nucleon channel represents the excitation of multinucleon channels. In the inclusive reaction, the latter also contributes to the cross section. A comparison of the inclusive cross section, obtained by (15), with that obtained in the DWIA treatment of the one-nucleon knockout (14a), gives the strength going into more complicated channels than the one-nucleon one.

One final remark concerning the distortion effects in processes (14a) and (14b) is in order. In the high-energy approximation to the optical potential, one implicitly classifies the processes according to the complexity of the nuclear states excited. Introduction of a final-state distortion in (14b) would be due to coupling to the 3p-3h channels. This leads to a consistent theory for the inclusive reaction, only if the same 3p-3h states appear as final state also. In our restricted formalism, distorted wave functions or Green's functions appear only in the 1p-1h subspace. We emphasize that this is precisely what is assumed in the first-order optical potential approximation to the high-energy projectile nucleus scattering.

We conclude this section by writing down the explicit expression for the inclusive (e,e') cross section, used in the present calculation. The basic quantity for the calculation is the response function obtained in the approximation (15)

$$\begin{aligned}
R_{p(n)}(\omega,q) &= \sum_h \int d^3x\, d^3x' e^{-i\vec{q}\cdot(\vec{x}-\vec{x}')} \\
&\quad \times \mathrm{disc}[iG(\vec{x}',\vec{x},\omega - |\epsilon_h|)\phi_h(x)\phi_h^*(x')]\,,
\end{aligned} \tag{16}$$

where G is the single-particle Green's function and the sum is over proton (neutron) occupied orbits. The cross section is given by

$$\frac{d^2\sigma}{d\Omega\, d\omega} = \frac{m}{m+\omega}\left[\sigma_{en} R_n(\omega,q) + \sigma_{ep} R_p(\omega,q)\right], \quad (17)$$

where $\sigma_{ep(n)}$ is proton (neutron) single-particle cross section (3). This factorization formula is equivalent to the nonrelativistic one with impulse charge current[10,3-5] in the quasifree region ($\omega \sim q^2/2m$), provided that the transverse convection current term is dropped and the spin correlation effect is neglected in the response function. The convection current contribution to the cross section is given near the quasifree peak

$$\delta\left(\frac{d^2\sigma}{d\Omega\, d\omega}\right)_{\text{conv}} = T_2(q_\mu{}^2)\left(2\tan^2\frac{\theta}{2} + \frac{|q_\mu{}^2|}{q^2}\right)\frac{k_F{}^2}{4m^2} \times R(\omega \approx \omega_{\text{peak}}, q_{\text{peak}}) \approx 0.025\, T_2(q_\mu{}^2) R(\omega \approx \omega_{\text{peak}}, q_{\text{peak}}), \quad (17a)$$

for an incident electron energy of 500 MeV and a scattering angle of 60°, the Stanford kinematics.[6] Thus the convection current contributes only a few percent throughout the energy region of our interest and is safely neglected for these kinematics. The contribution from the spin-orbit current vanishes up to $O(q^2/m^2)$ for the L-S closed shell nuclei, if the spin-dependent final state interaction is neglected. Therefore, we expect this factorization approximation to be valid for quantitative comparison with experimental data at the Stanford kinematics.[6] In this approximation, the only dynamical quantity involved is the Coulomb response function, and this considerably simplifies the numerical calculation.

III. QUASIFREE ELECTRON SCATTERING AT HIGH ENERGY

In this section, we apply the formalism outlined above to the 500 MeV (e,e') data[6] at 60°. For these data, the energy of the outgoing nucleon in the quasielastic peak is about 100 to 150 MeV. These data have been used in the past to extract, within a nuclear matter framework, the Fermi momentum.[6,11,12] Our aim is first to study to what extent these data can be interpreted using the existing information on the nuclear ground state from elastic electron scattering, and on the final-state interaction from nucleon-nucleus scattering. Second, we shall discuss in detail the influence of the final-state interaction on the inclusive cross section, particularly the role of the optical potential, and calculate the cross section corresponding to multinucleon removal.

We now specify the input necessary for the calculation of the response function in the single-particle approximation (16). For the description of the ground-state single-particle wave function ϕ_i, harmonic oscillator (HO) wave functions have been used. The oscillator parameters b_i are obtained either from electron scattering, or, for the medium-heavy nuclei, from the HO expansion of the Hartree-Fock wave functions of Ref. 13. With the exception of ^{6}Li, the small variations of the oscillator parameters, corresponding to different shells, leads to very small modifications of the quasielastic cross section. The single-particle Green's function has to be calculated at the energy

$$\omega_i = \omega - \epsilon_i, \quad (18)$$

where ϵ_i is the separation energy corresponding to the orbit i. The separation energies are taken from the $(e,e'p)$ experiments, when available, or extrapolated from the latter. The ground-state parameters ϵ_i, b_i are given in Table I.

The single-particle Green's function $G(i)$ is defined in the usual way:

$$G(i) = \left(\omega_i - \frac{q^2}{2Am} - \frac{p_i{}^2}{2\mu} - V_c(i) - u(i)\right)^{-1}, \quad (19a)$$

TABLE I. Harmonic oscillator parameters b and the binding energies of the single-particle neutron (n) and proton (p) orbits used in this work. The parameter b is related to that used in the shell-model analysis b_{SM} by $b = b_{\text{SM}} \times A/(A-1)$, A being the target mass number.

Nucleus	Orbit	b (fm)	Binding energy of single-particle orbit (MeV) n	p
^{4}He	0s	1.64	21.0	20.0
^{6}Li	0s	2.11	26.0	25.0
	0p	2.34	5.7	4.7
^{12}C	0s	1.69	40.9	38.0
	0p		20.2	17.5
^{24}Mg	0s		52.0	47.0
	0p	1.88	25.0	20.0
	0d		19.0	14.0
^{40}Ca	0s		63.3	56.0
	0p	1.97	48.8	41.5
	0d		22.2	14.9
	1s		18.5	11.2
^{58}Ni	0s	2.03	71.2	62.0
	0p		54.2	45.0
	0d		30.2	21.0
	1s		23.9	14.7
	0f		18.5	9.3

describing the relative motion of the knocked-out nucleon and the residual nucleus at the energy in the CM system

$$\epsilon = \omega_i - \frac{q^2}{2Am}. \tag{19b}$$

For knocked-out protons, $V_c(i)$ is the Coulomb potential corresponding to a uniform charge distribution

$$V_c(i) = \frac{Ze^2}{R}\left[\frac{3}{2} - \frac{1}{2}\left(\frac{r}{R}\right)^2\right], \quad r \leq R$$
$$= \frac{Ze^2}{r}, \quad r \geq R \tag{19c}$$

with the equivalent uniform radius R. μ is the nucleon—$(A-1)$ residual nucleus reduced mass:

$$\mu = \frac{A-1}{A} m ; \tag{19d}$$

$u(i) = u[\omega_i - q^2/(2Am)]$ is the energy-dependent optical potential.

The actual calculations of the Green's function is performed in an angular momentum basis and in coordinate space, neglecting L-S splitting:

$$\langle r' | G(i) | r \rangle = \sum_{lm} Y^*_{lm}(\hat{r}') g_l(r', r) Y_{lm}(\hat{r}) . \tag{20}$$

In the calculation of the radial Green's function $g_l(r, r')$, we have assumed that the optical potential is local and, therefore, expressible in terms of the regular and irregular wave functions. (Its explicit formulas are given in the Appendix.) Although the assumption of locality is not neccessary in our approach, very little is known about the details of the nonlocality of the optical potential. Even with this simplifying locality assumption, the numerical evaluation of the response function is rather tedious. For the response function of ^{40}Ca, for instance, about one hundred radial Green's functions are needed to calculate one point of the response function.

We have chosen the parametrization of Engelbrecht and Fiedeldey[14] for the local equivalent, energy-dependent optical potential. It consists of a central real part, a volume and a surface absorption terms. The last term has practically no influence at the nucleon energies relevant to this section. The potential is fitted to the nucleon-nucleus scattering data up to about 200 MeV, and connects smoothly to the ground-state shell-model potential.

We now discuss the use of this optical potential to calculate the quasielastic electron scattering cross section. As an example, we compare, in Fig. 1, our calculation with the ^{40}Ca data. For the nuclei Mg, Ca, and Ni, the calculation systematically overshoots the experimentally observed cross section. To trace the origin of this failure, we have calculated the energy integral over the response function for fixed momentum transfer of q equal to 450 MeV/c, which roughly corresponds to the momentum transfer at the quasielastic peak of the Stanford experiment. We have actually found a violation of the sum rule by about 5 to 10%. The cause of this failure is the following: In the above discussion of the sum rule in the high-energy approximation to the optical potential, we explicitly used the fact that the optical potential has singularities only on the real axis, thus satisfying an once-subtracted dispersion relation:

$$\mathrm{Re}\,u(\omega) = \mathrm{Re}\,u(0) + \frac{\omega}{\pi} \mathrm{P} \int_0^\infty \frac{\mathrm{Im}\,u(\omega')}{(\omega' - \omega)\omega'} d\omega' . \tag{21}$$

In contrast to the theoretical optical potential, our phenomenological optical potential does not satisfy the dispersion relation (21). It is interesting to note that quasielastic electron scattering is apparently sensitive to the analytic structure of the optical potential.

In order to restore the analytic properties of the

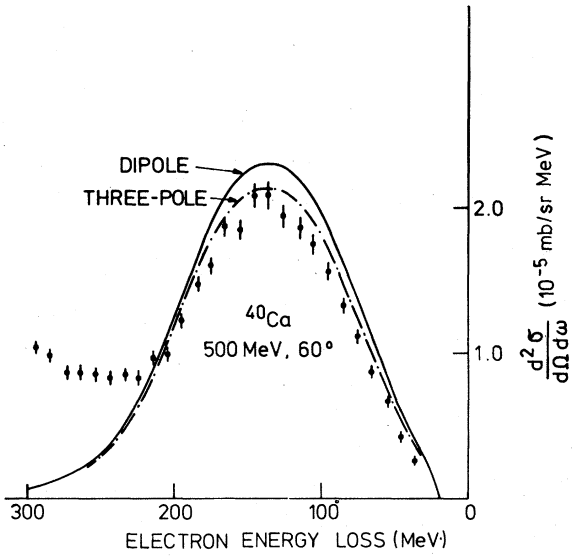

FIG. 1. Inclusive electron scattering cross section (in mb/sr MeV) for the incident electron energy of 500 MeV and a scattering angle of 60°, for ^{40}Ca, plotted against the nuclear energy loss (in MeV). Experimental points are from Whitney *et al.* (Ref. 6). Theoretical calculations use a dipole fit (solid line) and a three-pole fit (dotted line) for the nucleon form factors (Refs. 16 and 17). Nucleon-nucleus final-state interaction is taken into account by the phenomenological complex optical potential, which does not, however, satisfy the dispersion relation (21). Notice that the predicted cross section exceeds the experimental value slightly at the peak.

optical potential, the momentum dependence of u and the true energy dependence have to be separated. For this, we use the results of Ref. 14. In Ref. 14 this separation has been carried out by assuming the imaginary part $W(\omega)$ to be purely energy dependent. Using the dispersion relation (21), the corresponding energy-dependent piece of the optical potential $V_1(\omega)$ is calculated and the remainder is then assumed to be purely momentum dependent, i.e.,

$$u(\omega,p^2)=V_1(\omega)+V_2(p^2)+iW(\omega)\,. \tag{22a}$$

We have approximated the momentum-dependent term (22) V_2 by a linear dependence

$$V_2(p^2)=V_2^0 f_v(r)+\frac{\alpha}{2}\frac{1}{2m}\left[p^2 f_v(r)+f_v(r)p^2\right], \tag{22b}$$

with $V_2^0=-28$ MeV, $\alpha=0.1$, and f_v being defined as follows:

$$f_v(r)=\left[1+\exp\left(\frac{r-R}{a}\right)\right]^{-1}; \tag{22c}$$

the parameters R and a in Eq. (22c) are chosen such that Eq. (22b) reproduces the numerical results of Ref. 14 for V_2, within a few MeV.

Using the standard procedure, the Green's function corresponding to the optical potential (22a) can be written in terms of the Green's function corresponding to a local potential and a "Perey factor"[15]:

$$g_l(r',r)=\left[1+\alpha f_v(r')\right]^{-1/2} g_l^{\mathrm{loc}}(r',r) \times\left[1+\alpha f_v(r)\right]^{-1/2}, \tag{23a}$$

when g_l^{loc} is the Green's function corresponding to the equivalent local potential (see 22a)

$$u(\omega)=V_1(\omega)+V_2(2\mu\omega)+iW(\omega)\,. \tag{23b}$$

In transforming the nonlocal potential (22) to an equivalent local potential, the radial dependence is modified in the surface. We have neglected these surface modifications, since they are taken into account partly by the phenomenological fit of Ref. (14). Apart from this last approximation to the surface terms, the resulting response function must, by construction, satisfy the sum rule; we actually find the sum rule in the calculation to be fulfilled within typically $\frac{1}{2}$ percent for all the nuclei considered.

In the previous analyses of quasielastic electron scattering, the problem of the analytic structure of the optical potential did not occur. This is a consequence of neglecting the absorptive piece of the optical potential. In such calculations, consistency with (21) requires the real potential to have no true energy dependence. In our model, the phenomenologically observed energy dependence is attributed, with similar weight, to an intrinsic momentum dependence and to an energy dependence arising from the dissipative effects of the coupling to excited states.

We present in Fig. 2 a comparison of our calculations with the (e,e') data for nuclei between ^{4}He and ^{58}Ni. In general, both the peak position and the peak value of the cross sections agree reasonably well with experiment. The peak position is sensitive to the value of the real part of the optical potential at the energy for which the asymptotic kinetic energy of the knocked-out nucleon is about 120 MeV. To obtain qualitatively the right peak position, the weakened attraction of the optical potential, as compared to the ground-state potential, is crucial [$\mathrm{Re}\,u(\omega\approx 120$ MeV$)\approx -20$ MeV]. Apart from the momentum distribution of the ground state, the peak value is influenced by the momentum dependence of the optical potential, represented by the parameter α of Eq. (22b) and (23a), and by the corresponding value of the imaginary part of $u(\omega)$.

A quantiative comparison between our calculations and the data indicates a shift of 2.5 MeV in the calculated peak positions towards lower energies. At such a level of accuracy, clearly a number of small effects play a role; kinematic corrections, such as relativistic corrections to the proton, or Coulomb distortion effects on the electron, are important. At the Stanford kinematics, and for the medium-heavy nuclei, the corresponding shifts in the peak position are of the order of 4 MeV, but of different sign. Therefore, the small discrepancy in the peak position most likely has a dynamical origin. Within our formalism, the largest uncertainty arises from the poorly known momentum dependence of the optical potential. To explain the discrepancy in such terms, a stronger momentum dependence for proton energies below the quasielastic peak would be needed. Another possibility to account for the shift would be to weaken further the attraction in the final state by about 5–10 MeV; however, this would be in conflict with the fits to nucleon-nucleus scattering.

For the medium-weight nuclei, our calculated peak intensities agree reasonably well with the experimental values. For the light nuclei, we systematically underestimate the peak intensity by about 5–10%. The uncertainty in the e-N form factor is typically 3% for the proton, and about 10% for the neutron.[16,17] This implies an uncertainty of about 8% in the (e,e') cross sections (Fig. 1). The remaining discrepancy may be attributed to our crude treatment of the nonlocality in the real part of the optical potential, which is more serious in the light systems. Uncertainties

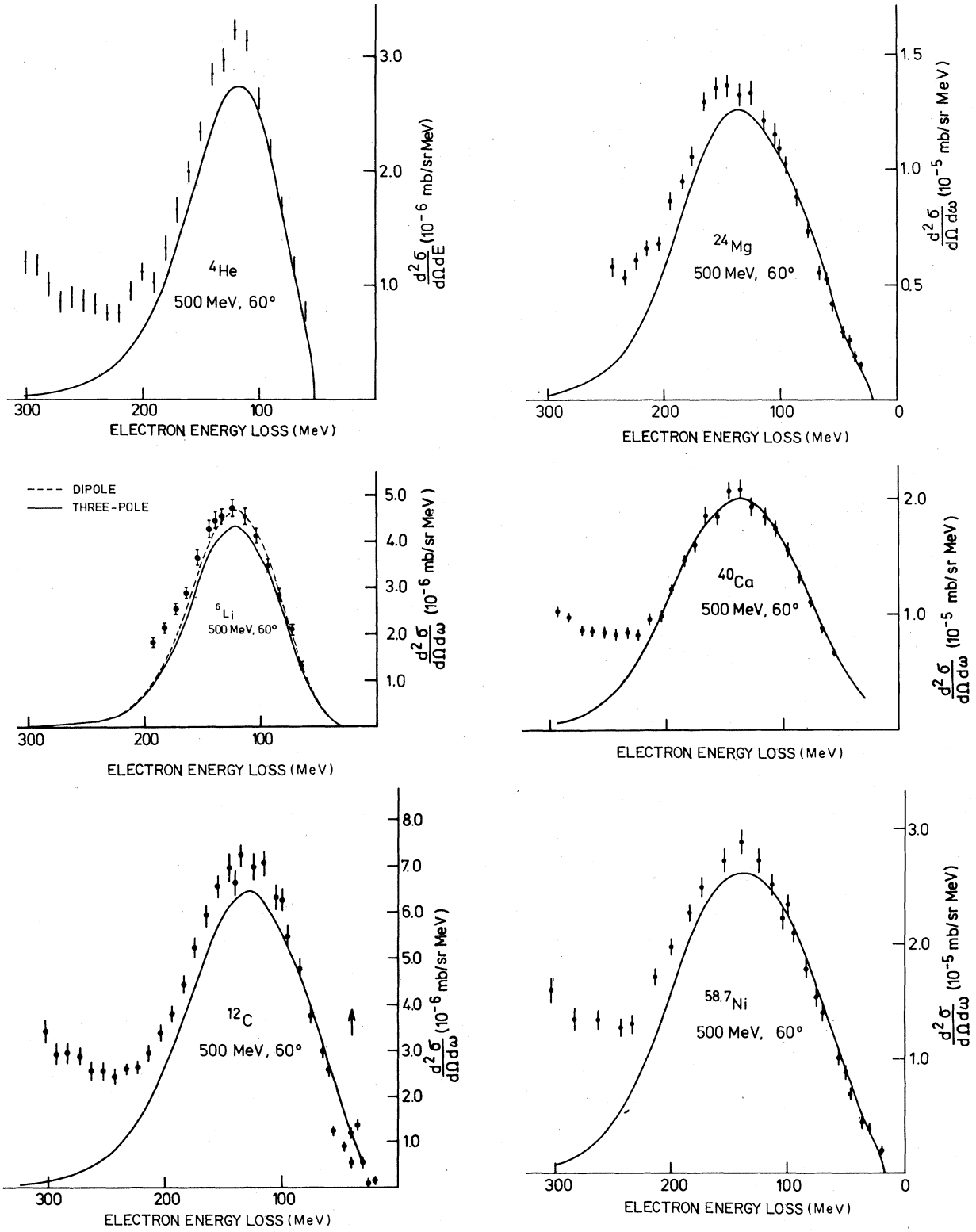

FIG. 2. Same as Fig. 1, for targets ^{4}He, ^{6}Li, ^{12}C, ^{24}Mg, ^{40}Ca, and ^{58}Ni. Data are from Ref. 6. Theoretical calculations now and hereafter take into account corrections due to the lack of proper analytic behavior of the phenomenological nucleon-nucleus optical potential. In this and the following figures, three-pole fit of the nucleon form factor is used, the exception being ^{6}Li, where the dipole fit is also shown, by the dotted line.

in the imaginary part are not important here.

The threshold behavior, i.e., the cross sections at small energy transfer, are correctly reproduced by using realistic values of the separation energies. For the very light nuclei it is important, because of the large momentum transfer, to take into account the recoil energy [cf. Eq. (19a)], which, for ^{4}He, is of order of 30 MeV. At the very-high-energy losses, our calculations, which do not include pion production, clearly fail to reproduce the data. We emphasize that, as compared to the nuclear matter calculations of Refs. 11 and 12, both finite size and final-state interaction effects reduce the discrepancy in the transitional region between quasielastic scattering and quasifree pion production. At an energy loss of 250 MeV, the pion production cross section in ^{12}C is about 0.8×10^{-6} mb/sr MeV, (Ref. 11) the quasielastic contribution calculated by us is 0.75×10^{-6}; these add up to about half of the experimentally observed cross section. For ^{40}Ca, the corresponding numbers at $\omega=260$ MeV are $\sigma_{(e,e'\pi)}=0.3$ mb/sr MeV (Ref. 11), $\sigma_{e,e'}=0.2$ mb/sr MeV, the sum of which is 60% of the observed value.

We now discuss the influence of the absorptive effects in the (e,e') reaction. In Fig. 3, we compare the full calculation (cf. Fig. 2) with one in which the imaginary part of the optical potential is turned off. The major effect of the imaginary part is to reduce the cross section around the peak by 5–10%, and to shift some of the strength towards the high-energy loss side. The integrated strength is clearly different in two cases. In contrast to the complex optical potential, the real "pseudopotential" takes care only of the dissipative effects arising from the coupling to more complex channels, and thereby violates the sum rule.

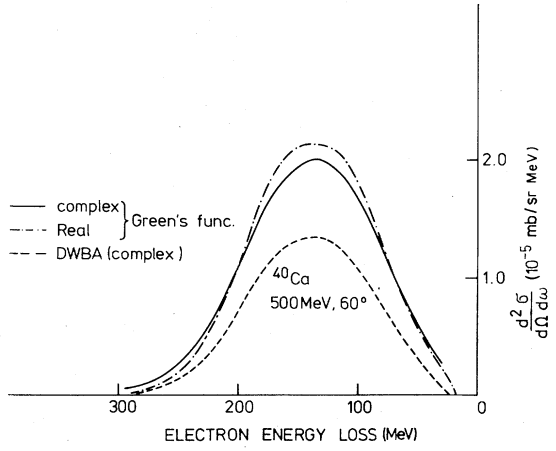

FIG. 3. Same as Fig. 2: ^{40}Ca. Solid curve uses a complex phenomenological nucleon-nucleus optical potential, while the dash-dot curve is obtained with a real one. Dashed curve shows the DWBA prediction.

Although the overall effect of the absorptive corrections is rather small, this does not imply that the contributions from more complicated channels are small. As the comparison with the DWIA calculation in Fig. 3 shows, about 40% of the inclusive (e,e') reaction in ^{40}Ca are due to multinucleon removals. This reduction of the 1p-1h excitation cross section can be understood qualitatively by calculating the probability for the knocked nucleon to escape from the nucleus without an additional interaction. Assuming a uniform matter distribution, this probability is given by

$$P_t=\frac{3}{8y^3}\left[2y^2-1+(1+2y)e^{-2y}\right], \tag{24a}$$

where

$$y=R/\lambda\,. \tag{24b}$$

R is the equivalent uniform radius; λ is the nucleon mean free path, related to the optical potential by

$$\lambda^{-1}=-\frac{2m}{p}\,\mathrm{Im}\,u\,, \tag{24c}$$

p being the nucleon momentum. At the quasifree peak, the estimate (24a) gives, with $y=0.8$,

$$P_t=0.59\,, \tag{24d}$$

for ^{40}Ca. This explains the reduction found in our DWBA calculation.

This semiquantitative argument shows immediately that, for a large nucleus, only the nucleon at the surface contribute to the 1p-1h excitation. Assuming $y\gg1$, we obtain

$$P_t\underset{y\gg1}{\longrightarrow}\frac{3}{4y}=\frac{3\lambda}{4R}\,. \tag{25}$$

Therefore, the energy integrated 1p-1h excitation cross section is proportional to

$$P_t\int R(q,\omega)\,d\omega=Z\cdot\frac{3\lambda}{4R}=\frac{3}{4}\frac{\lambda}{r_0}Z^{2/3}\,, \tag{26}$$

with $R=r_0Z^{1/3}$. In such a situation, quasielastic electron scattering is dominated by multinucleon removal ($\propto Z$).

We now give a quantitative argument why the appreciable multinucleon removal has a rather small effect on the inclusive (e,e') cross section. Neglecting the energy dependence of the imaginary part, the response function can be written as a folding of the polarization propagator for a real final-state interaction π_0, with the Lorentzian modulation due to the absorption

$$R(q,\omega)\propto\mathrm{Im}\,\frac{1}{2i\pi}\int_{-\infty}^{+\infty}d\omega'\,\frac{1}{\omega'-\omega-i\,\mathrm{Im}\,u}\,\pi_0(q,\omega')\,. \tag{27}$$

In this form, it is obvious that the effect of the absorption is determined by the energy variations of the Lorentzian and the polarizon propagator π_0. To make this explicit, we evaluate $R(q,\omega)$ by using, for π_0 in (27), the noninteracting Fermi-gas approximation ($q > 2k_f$):

$$\pi_0(q,\omega) \propto \int_0^{k_f} d^3k \frac{1}{\omega - \frac{(\vec{k}+\vec{q})^2}{2m} + \frac{k^2}{2m} + i\epsilon}. \tag{28}$$

At the quasi-elastic peak ($q^2 = 2m\omega$), we obtain, for the modification due to absorption [$R_0(q,\omega) = \mathrm{Im}\pi_0(q,\omega)$]:

$$\frac{R(q,\omega)}{R_0(q,\omega)} \approx \left(1 - \frac{4}{\pi\sqrt{2}} \frac{|\mathrm{Im}u|}{\Gamma_F/2}\right), \tag{29a}$$

where

$$\Gamma_F = \sqrt{2}\,\frac{k_f q}{m} \tag{29b}$$

is the full width at the half-maximum of the Fermi-gas response function. In this model, the smearing of a sharp response [$\delta(\omega - q^2/2m)$] is due to two causes: (1) the momentum uncertainty due to Fermi motion, the corresponding distribution of which is characterized by $\Gamma_F/2$, and (2) the uncertainty due to the lifetime of the excited particle-hole states, given by $\mathrm{Im}u$. For ^{40}Ca and the Stanford kinematics ($k_f = 250$ MeV/c, $q = 450$ MeV/c), we find, with Eqs. (29), a 9% reduction of the peak intensity due to absorption, which agrees with our full calculation. Thus, for these kinematics, the peak intensity is primarily determined by the momentum distribution in the ground state. For larger-energy transfer, the optical potential can be calculated from N-N scattering:

$$-2m\,\mathrm{Im}u = 4\pi\rho\,\mathrm{Im}f = p\sigma_{\mathrm{tot}}\rho \tag{29c}$$

where f and σ_{tot} are the N-N forward amplitude and total cross section, respectively, at the energy $\omega = p^2/2m$. The reduction of the quasielastic peak (29a) is now given by

$$\frac{R(q,\omega)}{R_0(q,\omega)} = \left(1 - \frac{4}{3\pi^3}\sigma_{\mathrm{tot}}k_f{}^2\right). \tag{29d}$$

Using the asymptotic value $\sigma_{\mathrm{tot}} = 40$ mb and $k_f = 1.35$ fm^{-1}, we find a 30% reduction. For high enough energies, N-N scattering is strongly inelastic, and the reduction calculated with (29d) is then partly due to pion production in the final-state interaction of the knocked-out nucleon.

It is interesting to observe that a 30% reduction of the quasielastic peak is inconsistent with the data at Stanford kinematics. Assuming that our ground-state momentum distribution is reasonable, this clearly shows that the optical potential at $\omega = 130$ MeV cannot simply be calculated from free N-N scattering ($\sigma_{\mathrm{tot}}^{pn} + \sigma_{\mathrm{tot}}^{pp} = 35$ mb at $\omega = 130$ MeV). This is in qualitative agreement with both phenomenological analyses and theoretical calculations of the optical potential. We stress that the quasielastic (e,e') reaction is an independent test of the imaginary part of the optical potential. In contrast to proton-nucleus scattering, which is a surface reaction, the (e,e') reaction probes the nuclear interior as well, and is thus, sensitive to the optical potential at nuclear matter densities.

Quantitatively, the value of the imaginary part of the optical potential, used in our calculation, is in disagreement with those derived from microscopic nuclear matter calculations.[18] The predicted value of the imaginary part, for nuclear matter density and energies around 100–150 MeV, is about 15–20 MeV, while in the parametrization[14] used here, the corresponding values are about 10 MeV. Such smaller values are also obtained in a fit to recent data.[19] Our results for the inclusive (e,e') data are not consistent with the "large" theoretical values of the imaginary part of the optical potential, unless the nonlocality in the real part is drastically changed. In Fig. 4, we show the results for the (e,e') cross section on ^{40}Ca with the standard choice of the optical potential and a potential with twice the imaginary part. In order to preserve the sum rule, the Perey factor α [Eq. (23)] has been reduced at the same time by a factor of 4. There is no signifi-

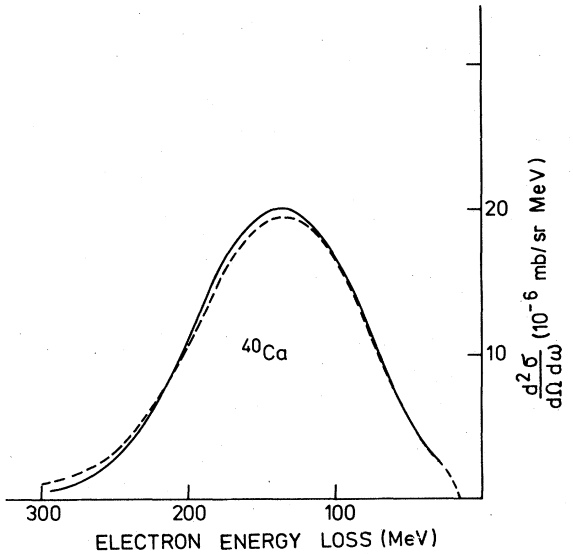

FIG. 4. Same as Fig. 2. Solid curve uses the standard final-state interaction potential for ^{40}Ca, the dashed curve has the imaginary part of the optical potential *twice* as large as the standard one at each energy. The Perey factor in the second case is reduced by a factor of 4, compared to the standard case.

cant difference in the two fits to the data. However, the last choice for the optical potential would not only be in disagreement with nucleon-nucleus scattering data, but also with the prediction of a much larger nonlocality in the nuclear matter calculations.[20]

The results of our calculation show that, using the available information on the nuclear ground state and the phenomenological optical potential, the Stanford inclusive data can be described adequately. This indicates strongly that, apart from nucleon self-energy insertions, there are no other important medium corrections for these kinematics. The dominance of the self-energy insertions is a familiar high-energy concept. It is tested, for instance, in the inelastic nucleon-nucleus scattering, where it allows us to take the optical potentials for the ground and excited states to be the same.

One obvious example of a medium correction, neglected above, is the 1p-1h rescattering, which is known to be important for low-energy processes. We now discuss it in some detail. Qualitatively we expect that, with increasing energy and momentum transfer, the corresponding 1p-1h form factors suppress these contributions, while the 2p-2h excitations by final state interaction are less hindered by the threshold factors, and hence will finally dominate. To make these arguments more quantitative, we now calculate, in a schematic way, the influence of particle-hole rescattering on the response function for the Stanford kinematics. In nuclear matter, the effect of the particle-hole interaction $u_0(q)$ is given, in the ring approximation, by

$$\mathrm{Im}\pi(q,\omega)=\mathrm{Im}\frac{\pi_0(q,\omega)}{1-u_0(q)\pi_0(q,\omega)}, \tag{30}$$

where $\mathrm{Im}\pi_0(q,\omega)$ is the free Fermi-gas response function.[21] We use Eq. (30), but with the finite-nucleus polarization propagator calculated above. In the region of the quasielastic peak, the finite nucleus and the nuclear matter response functions are not too different. Therefore, this prescription should be reasonable. In Fig. 5, the response functions, obtained with and without particle-hole rescatterings, are compared. For $u_0(q)$, we have used a zero-range Migdal parametrization with the empirical values of the parameters quoted in Ref. 22. The main effect of the particle-hole interaction is to shift the quasielastic peak towards larger energy losses. The peak intensity, however, is unaffected. The shift in the peak is directly related to the repulsive nature of the particle-hole interaction. Its value of 20 MeV cannot be taken seriously at all, since the Migdal parameters used are appropriate only

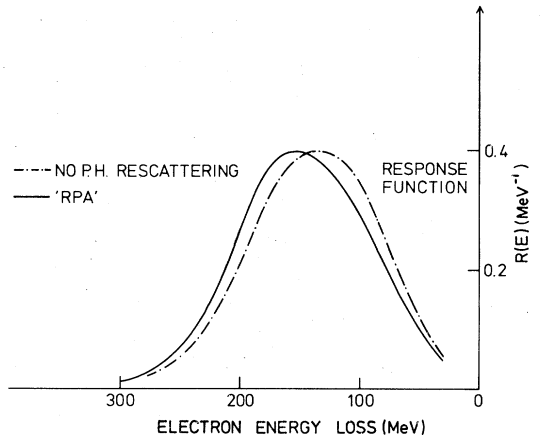

FIG. 5. Response function for the Stanford kinematics (Ref. 6) for ^{40}Ca without particle-hole (p-h) rescattering (dash-dot line) and with p-h the rescattering (RPA) correction (solid line). The plotted response function has a normalization $(1/\pi)\int_0^\infty R(E)\,dE=Z$, Z being the number of target protons.

for processes close to the Fermi surface, and not for processes involving momentum transfer as large as 450 MeV/c. From our analysis, we expect that the repulsion at these momentum and energy transfer should be at least a factor of 4 smaller. The equality in the peak intensity is due to the fact that the particle-hole force used has no imaginary part. This, together with the fact that the real part of the polarization propagator vanishes close to the quasielastic peak, leaves the peak intensity unchanged to lowest order in the particle-hole interaction.

From a comparison of our calculations to the data, we can get a qualitative bound on a possible imaginary part in the particle-hole force. Allowing for a 5% change in the peak intensity we find

$$|\mathrm{Im}F_0| \quad \text{and} \quad |\mathrm{Im}F_0'| \leq 0.1\,. \tag{31}$$

($F_0'=0.7$, in the parametrization[22].) The particle-hole rescattering just discussed is one of the possible medium corrections, in addition to the self-energy insertions. The smallness of the correction in the quasielastic peak is not specific for this particular process. It can be expected on the basis that the knocked-off nucleon can propagate on the energy shell in the quasielastic peak, as is indicated by the purely imaginary polarization propagator. In such a situation, no interaction is required to balance energy and momentum of the nucleon. Away from the quasielastic peak, the nucleon can propagate only over a finite distance d without additional interaction. From the uncertainty principle, we get

$$d=\nu/\Delta E\,, \tag{32a}$$

with

$$\nu = q/m, \quad \Delta E = \omega - q^2/2m . \tag{32b}$$

With increasing ΔE, the medium has to supply more and more momentum to the nucleon. Once d becomes comparable to the internucleon distance ($d \sim 1.5$ fm, $\Delta E \sim 70$ MeV, for the Stanford kinematics), away from the quasielastic peak, detailed off-shell properties of the optical potential can be expected to be important. Finally, if d becomes comparable to the dynamical correlation length ($d \sim 0.5$ fm, $\Delta E \sim 200$ MeV), the single-particle description must fail.

IV. LOW-ENERGY (e,e') SCATTERING AND RADIATIVE π CAPTURE

Here we apply our formalism for inclusive reactions to kinematical situations where both energy and momentum transfer are not large anymore on the nuclear scale. In this regime, medium corrections other than the final-state interaction, described by the optical potential, are expected to be important as well. By comparing our calculations with the experimental data, we want to explore the importance of these corrections.

In Fig. 6, the data of Ref. 7 are compared with our calculations. The typical momentum transfer here is about 90 MeV/c. The calculation, without surface absorption in the phenomenological optical potential, shows a very strong peak at an excitation energy of about 22 MeV, corresponding to a d-state single-particle resonance. The structure seen around 40 MeV is also due to a d-state resonance, but with the nucleon removed from the s shell. The occurrence of these sharp resonances

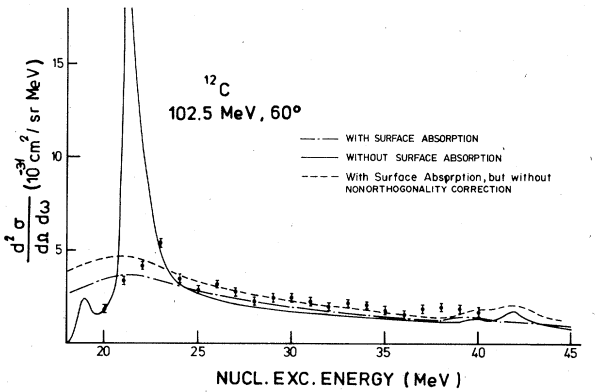

FIG. 6. ^{12}C. Inclusive electron scattering by ^{12}C for the incident electron energy of 102.5 MeV and a scattering angle of 60°; solid line, without surface absorption in the final-state interaction potential, dash-dot line, with it. The curve with the dashed line contains surface absorption, but is without the nonorthogonality correction. Notice the strong damping of the single-particle resonance in the second case. The experimental data are from Ricco *et al.* (Ref. 7).

is a consequence of our single-particle description of the nucleus, and has been noted in similar calculations before.[4] The volume absorption at the corresponding particle energies of about 5 MeV is not strong enough to damp these peaks.

As Fig. 6 shows, the surface absorption term in the phenomenological optical potential, which is unimportant in the high-energy data, changes drastically the structure of the cross section at low excitation energies. Although a reasonable damping of the single-particle resonance is achieved, the physical interpretation of the underlying damping mechanism is much less transparent than that for the volume absorption. The coherent particle-hole rescattering, described within the framework of the random-phase approximation (RPA), is completely ignored in our calculation. It is known that this rescattering mechanism strongly influences the low-energy loss side of the nuclear response function. With increasing energy transfer to the nucleus, the response shows less structure, and is reasonably well represented by our calculation. The data even indicate a structure around 40 MeV, related to the threshold for the removal of s-shell nucleons. As Fig. 6 shows, the surface absorption damps the $l=2$ resonance completely, without disturbing the threshold effects. Additional damping may be expected here due to the s-shell hole width, not included in our calculation. In the light- and medium-weight nuclei considered above, the small statistical weight of the deeply bound nucleon makes the broadening of the response function due to the hole width less important than that due to the particle width.

Although the shape of the experimental spectrum at high excitation energies seems to be described well by our single-particle model, there are basic theoretical difficulties which may make this agreement less compelling. As an example of these difficulties, we mention the lack of orthogonality in the wave functions implied by the energy dependence of the optical potential. To estimate this effect, we subtract from the single-particle propagator its components in the occupied states, i.e.,

$$\tilde{G} = G - \sum_{\alpha,\beta} |\alpha\rangle \langle\alpha|G|\beta\rangle \langle\beta| , \tag{33}$$

where α and β run over the occupied states. This, by construction, has the property to make the cross section vanish for $q \to 0$ at finite energy transfer. Because of the high momentum transfers involved in the Stanford experiment,[6] the resultant corrections are unimportant ($\lesssim 1\%$) over the entire energy loss spectrum. However, for the low-energy data, the kinetic energy of the outgoing nucleon is comparable to the potential ener-

gy. Therefore, the difference between the potentials for ground state and final state, respectively, leads to an appreciable orthogonality defect, as seen in Fig. 6. These effects are particularly important when the absorptive surface potential is included. In contrast to the volume term of the optical potential, the surface absorption makes the optical potential appreciably different from the ground-state potential even near the threshold.

Summarizing the above discussion, we emphasize that, for low excitation energies, our description of the nuclear excited states is too poor to reproduce the detailed structure of the response function. On the high-energy side, the calculations agree quite well with the data. Unfortunately, the electron scattering data do not go far enough in excitation energy. It is, therefore, not clear whether the 10–20% underestimate of the strength in the tail around 40 MeV indicates a failure of our single-particle description. In radiative pion capture reactions ($\pi^- A \to \gamma + X$), this kinematical region of high-energy loss and comparatively low momentum transfer is covered. Below we apply our formalism to the $\pi^- - {}^6\mathrm{Li} \to \gamma + X$ reaction. We have chosen this nucleus, because the $1S$ radiative capture process in this target has been separated from the $2P$ capture by the recent coincidence experiment.[8] From our point of view, the $1S$ capture process is preferable, because here we avoid the theoretical uncertainties of the momentum-dependent terms in the capture Hamiltonian,[23] and uncertainties in the pionic wave function resulting from the strong p-wave pion-nucleus optical potential. The differential capture rate is given by[24]

$$\frac{d\Gamma^{\gamma}_{1S}}{dE_{\gamma}} = \frac{\alpha g^2}{m^2}\frac{E_{\gamma}}{m_{\pi}}\left(1+\frac{m_{\pi}-E_{\gamma}}{m}\right)^{-1}(\alpha Z m_{\pi})^3/\pi \times F_{\mathrm{corr}} \cdot R(E_{\gamma}, m_{\pi}-E_{\gamma}), \tag{34}$$

with $g^2/4\pi = 14.28$, and $(1/\pi)(\alpha Z m_{\pi})^3 F_{\mathrm{corr}}$ is the pionic density at the origin. $F_{\mathrm{corr}} = 0.70$ (Ref. 25) corrects for the finite size of the nuclear charge distribution.

In Fig. 7, we compare our calculations with the experimentally observed inclusive gamma spectrum. The figure shows the effects of the surface absorption term in the phenomenological optical potential and the overlap correction [Eq. (33)]. We first note that neither of these corrections has significant effect on the integrated radiative branching ratio, which is found to be

$$\Gamma^{\gamma}_{1S}/\Gamma^{\mathrm{abs}}_{1S} = (3.32 \pm 0.15) \times 10^{-2}, \tag{35}$$

where the uncertainty reflects the modifications due to these corrections. Its experimental value, for transitions to the excited state of ^{6}He, is[8]

$$\Gamma^{\gamma}_{1S}/\Gamma^{\mathrm{abs}}_{1S}(\mathrm{exp}) = (4.11 \pm 0.55) \times 10^{-2}. \tag{36}$$

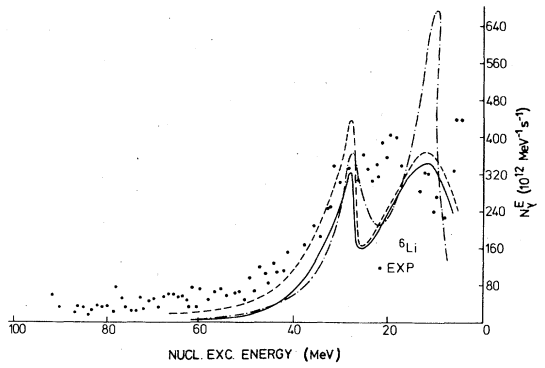

FIG. 7. Inclusive photon spectrum from the radiative capture of pions in the $1S$ atomic state of ^{6}Li. Experimental data are from the Lausanne-Munich-Zurich collaboration (Ref. 8). Theoretical calculation shows three cases. (1) Solid line: with nonoverlap correction. (2) Dashed line: without nonoverlap correction. (3) Dash-dot line: with nonoverlap correction, but without the surface term in the optical potential.

Not shown in the Fig. 7 is the contribution of a discrete transition to the response function. This corresponds to a single-particle state with the configuration $(0p, 0s^{-1})$, and carries 25% of the integrated strength. As in the case of the low-energy electron scattering in ^{12}C, the two peaks correspond to d-wave single-particle resonances, with the proton removed either from the p or the s shell. Again, the detailed structure of the spectrum at low excitation energies is sensitively influenced by the surface absorption term. Here, we must doubt even more the damping mechanism provided by the phenomenological surface term, due to rather low level density in ^{6}He at the corresponding excitation energies. Clearly, a microscopic description of the spreading of the strength due to the residual interaction is required. The treatment of the residual interaction within a shell-model bound state calculation[26] for ^{16}O indicates that a spreading of the strength within, typically, 5–10 MeV is to be expected. However, the corresponding strength, which is concentrated in our model in the single-particle resonances, should not be altered appreciably by the residual interaction. To add resonance contributions to the quasifree process, as done in the Ref. 26, certainly contains double counting. Our qualitative agreement in the branching ratio with the experimental value suggests that the overestimate in the Ref. 26 is at least partly due to this double counting.

At high-energy transfers to the nucleus, the radiative capture displays the limitations of our approach away from the quasifree region (quasielastic electron scattering data for this regime are lacking). First, we note that the experimen-

tal data fall off more gradually, with increasing energy transfer, than predicted. Second, the large overlap corrections indicate important two-nucleon mechanism, apparently not taken into account in an appropriate manner by the phenomenological optical potential. Finally, it must be kept in mind that, with increasing energy transfer to the nucleus (i.e., large momentum transfer to the nucleon), the harmonic oscillator ground-state wave function may not provide enough high Fourier components. Note that, at 60 MeV, the initial s-nucleon momentum required is 280 ± 80 MeV/c, if final-state interaction is neglected.

We conclude this section with a brief discussion of the recent Saclay data.[27] In this experiment, the (e,e') inclusive cross section has been measured for several incident electron energies ranging from 280 to 520 MeV at 60° and 130°. In Fig. 8, we compare our prediction with the data for 480 and 400 MeV incident energies. As for the Stanford data, our prediction agrees quite well with the 480 MeV data. For lower energies, the experimental cross sections are systematically lower. The ratio in the peak intensity between theory and experiment is 0.98, 1.08, 1.21, and 1.18, at the incident energies of 480, 440, 401, and 360 MeV, respectively. Also at the lower energies, we systematically overestimate the cross sections at the quasielastic peak. However, as this peak overlaps with single-particle resonances in our model, such a quantitative comparison does not make sense. Discrepancies in the quasielastic peak up to 30% are impossible for us to understand in terms of final-state interaction, which, as discussed above, gives rise to typically 10% corrections. An increase in the imaginary part of the optical potential by a factor of 3 to 4 would be necessary to accommodate the observed inclusive cross section at 400 MeV obtained at Saclay. The energy dependence of the discrepancy is equally disturbing. Obviously, the reduction of the peak intensity must decrease with decreasing nucleon energy and, therefore, indicates a corresponding weakening of the imaginary part of the optical potential. The experiment, however, would suggest the opposite trend. On the other hand, we cannot see any other medium corrections which would lead to a strong energy dependence in the cross section between 500 and 400 MeV incident electron energy, but would restore the qualitative agreement for the 102 MeV data discussed above. Comparison of the Stanford data and the Saclay data at 400 MeV for the same energy losses suggests a 30% variation of the response function beyond our prediction in a range of momentum transfers of 100 MeV/c. Thus, the Stanford and Saclay data, taken together, would suggest a strong dependence of the response function in both energy and momentum, far beyond our model.

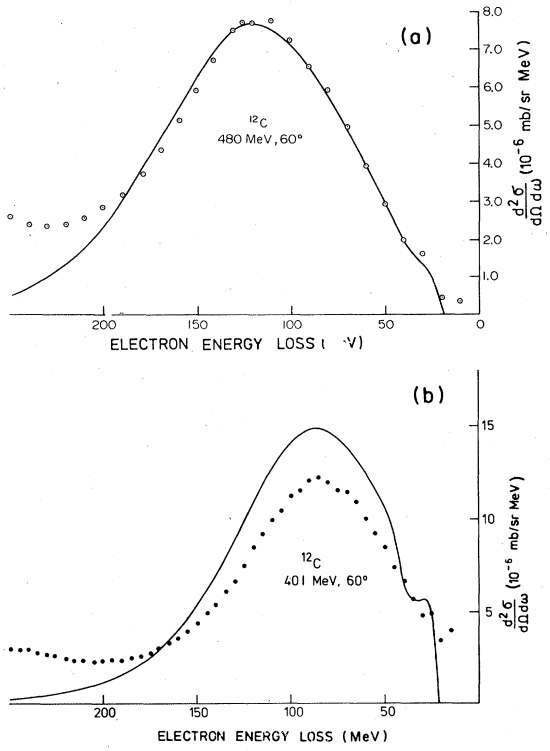

FIG. 8. Inclusive electron scattering by ^{12}C at 60° with incident electron energies of 480 MeV (a) and 401 MeV (b). Theoretical predictions are represented by the solid line. Experimental data are from the Saclay group (Ref. 27).

V. CONCLUSION

We have discussed in the present paper the problem of final-state interaction in inclusive electromagnetic processes in which the final nuclear states are not observed. In contrast to the exclusive $(e,e'p)$ reaction, the inclusive (e,e') reaction cannot be described within a DWBA formalism. The DWBA treatment accounts only for the attenuation of the flux in a given channel, as is appropriate for the $(e,e'p)$ process. It, however, cannot account for the corresponding excitation of other channels, and is therefore, not appropriate for inclusive processes. We have shown here that their proper description is provided by the Green's function formalism. Like DWBA, it is a single-particle theory. But, unlike DWBA, it accounts for both the loss of flux out of the primary channel and the corresponding gain in the secondary (multiparticle removal) ones. We have

shown, in the high-energy approximation for the optical potential, that the loss of flux in the 1p-1h channel is compensated, as far as the sum rule is concerned, by the excitation of the 2p-2h states. In the actual analysis, we have used phenomenological optical potentials. In this case, certain analytic properties of the energy dependence of the optical potential have to be imposed to guarantee the sum rule. It is interesting to see that the (e,e') data considered are actually sensitive to such general analytic properties of the optical potential.

We have centered our discussion of the final-state interaction around the Stanford data. The main effect of the final-state interaction is to broaden the nuclear response function. The final-state interaction reduces the peak intensities for medium-heavy nuclei by typically 5–10%. Despite the comparatively small size of the effect, almost half of the cross sections goes to channels more complex than the primary one-particle one-hole ones. The comparison of our calculations with the Stanford data shows that the nuclear response function in the corresponding kinematic region can be described within a single-particle model, in which the known properties of the nuclear ground state and the final-state interaction are used as inputs.

In order to find evidence for deviations from the single-particle model, we have extended our calculations of the nuclear response function to processes at lower four-momentum transfers. The gross features of these can be understood within our model. However, the detailed structure at very-low-energy transfer is not reproduced correctly. The single-particle model introduces resonance structures, the strength of which can only be distributed by considering the residual interactions. At comparatively high-energy and small momentum transfers, a regime covered by the radiative π capture, for instance, our model response function falls faster than what is experimentally observed.

Finally, we have compared our calculations with the recent Saclay (e,e') data for ^{12}C. On the basis of our analysis, the Stanford 500 MeV data and the 480 MeV Saclay data are incompatible with the Saclay data at lower incident electron energies. To explain both sets of data, a strong momentum and energy dependence of the response function would be required, far beyond any single-particle model.

ACKNOWLEDGMENTS

We thank Ingo Sick and Peter Truöl for supplying us with unpublished data. We are grateful to John Negele and Ingo Sick for valuable discussions. We acknowledge many stimulating exchanges with members of the SIN Theory Group.

APPENDIX

The radial Green's function for the optical potential $v(z)$ is given by

$$g_l(r,r',z) = -\frac{\phi_l(v(z),p,r_<)\chi_l^\dagger(v(z),p,r_>)}{p f_l(v(z),p)}, \quad \text{(A1a)}$$

$$p=(2\mu z)^{1/2}, \quad \mathrm{Im}(2\mu z)^{1/2}\geq 0, \quad \text{(A1b)}$$

where ϕ_l, $\chi_l^\dagger$, and f_l are the regular, irregular, and Jost functions of the radial Schrödinger equation:

$$\left[\frac{d^2}{dr^2}-\frac{l(l+1)}{r^2}-v(r,z)+p^2\right]u_l=0. \quad \text{(A2)}$$

Note that

$$\begin{aligned}&\phi_l(v,p,r)\xrightarrow[r\to 0]{}\hat{j}_l(pr),\\ &\chi_l^\dagger(v,p,r)\xrightarrow[r\to\infty]{}h_l(pr),\\ &f_l(v,p)=\frac{1}{p}W[\chi_l^\dagger(v,p,r),\phi_l(v,p,r)],\end{aligned} \quad \text{(A3)}$$

W being the Wronskian; $\hat{j}_l$ and $\hat{h}_l^\dagger$ are the Riccati-Bessel and Riccati-Hankel functions, respectively. The physical outgoing solution $\phi_l^\dagger$ is related to ϕ_l by

$$\phi_l^\dagger(v,p,r)=\frac{\phi_l(v,p,r)}{f_l(v,p)} \quad \text{(A4)}$$

and g_l can also be written

$$g_l=-\frac{\phi_l^\dagger(v,p,r_<)\chi_l^\dagger(v,p,r_>)}{p}. \quad \text{(A5)}$$

Taking into account the nonorthogonality corrections [Eq. (33)] the particle Green's function g_l^P is given by

$$g_l^P(\omega)=g_l(\omega)-P_l g_l(\omega)P_l, \quad \text{(A6a)}$$

$$P_l=1-\sum_{l=h}|\phi_h\rangle\langle\phi_h|. \quad \text{(A6b)}$$

Explicit forms of the nuclear polarization operator, $\pi(q,\omega)$, used in our numerical calculation for closed shell nuclei, is given below:

$$\pi(q,\omega)=\sum_{\substack{l,l_g,j_g\\ l_h,j_h}}\int dr\,dr'(2l+1)(2l_h+1)(2j_h+1)(2j_g+1)C^2(l\,l_h l_g;0,0,0)W^2(ll_h j_g\tfrac{1}{2};l_g,j_h)$$
$$\times\hat{j}_l(qr)\hat{j}_l(qr')R_{l_h j_h}(r)R_{l_h j_h}(r')\frac{2\mu}{q^2}g_l^P(r,r',\omega-\epsilon_h), \quad \text{(A7)}$$

where C and W are Clebsch-Gordan and Racah coefficients, $R_{l_h j_h}(r)$ is the nuclear single-particle radial wave function, and ϵ_h is the binding energy of the occupied orbits. For nonclosed shell nuclei, such as ^{6}Li and ^{58}Ni, the result must be corrected to take properly into account the occupation number for the last orbit.

---

*Permanent address: Physics Laboratory, Juntendo University, Narashino-Fujisaki, Chiba, Japan.

[1]K. Nakamura and N. Izutsu, Nucl. Phys. A259, 301 (1975); K. Nakamura, S. Haramatsu, P. Kamae, H. Muramatsu, N. Izutsu, and Y. Watase, *ibid.* A268, 381 (1976).

[2]J. Mougey, M. Bernheim, A. Bussière, A. Gillebert, Phan Xuan Hô, M. Priou, D. Royer, I. Sick, and G. J. Wagner, Nucl. Phys. A262, 461 (1976).

[3]T. de Forest, Jr., Nucl. Phys. A132, 305 (1969).

[4]T. W. Donnelly, Nucl. Phys. A150, 393 (1970).

[5]Y. Kawazoe, G. Takeda, and H. Matsuzaki, Prog. Theor. Phys. 54, 1394 (1975).

[6]R. R. Whitney, I. Sick, F. R. Ficenec, R. D. Kephart, and W. P. Trower, Phys. Rev. C 9, 2230 (1974); J. S. McCarthy, I. Sick, R. R. Whitney, and M. R. Yearian, *ibid.* C 13, 712 (1976).

[7]G. Ricco, H. S. Kaplan, R. M. Hutcheon, and R. Malvano, Nucl. Phys. A114, 685 (1968).

[8]D. Renker, W. Dahme, W. Hering, H. Panke, Č. Zupančič, C. Alder, B. Gabioud, C. Joseph, J. F. Loude, N. Morel, J. P. Perroud, A. Perrenoud, M. T. Tran, E. Winkelmann, G. Strassner, and P. Truöl, Phys. Rev. Lett. 41, 1279 (1978); P. Truöl, private communications.

[9]A. E. L. Dieperink and T. de Forest, Jr., Annu. Rev. Nucl. Sci. 25, 1 (1975); A. E. L. Dieperink, T. de Forest, Jr., I. Sick, and R. A. Brandenberg, Phys. Lett. 63B, 261 (1976); S. Boffi, C. Giusti, F. D. Pacati, and S. Faullani, Nucl. Phys. A319, 461 (1979).

[10]K. M. McVoy and L. Van Hove, Phys. Rev. 125, 1034 (1961).

[11]E. J. Moniz, Phys. Rev. 184, 1154 (1969).

[12]F. A. Brieva and A. Dellafiore, Nucl. Phys. A292, 445 (1977).

[13]J. W. Negele and D. Vautherin, Phys. Rev. C 5, 1472 (1972); 11, 1031 (1975); J. W. Negele and G. Rinker, *ibid.* 15, 1499 (1977).

[14]C. A. Engelbrecht and H. Fiedeldey, Ann. Phys. (N.Y.) 42, 262 (1967); H. Fiedeldey and C. A. Engelbrecht, Nucl. Phys. A128, 673 (1969).

[15]F. G. Perey, in *Direct Reactions and Nuclear Reaction Mechanisms*, edited by E. Clementel and C. Villi (Gordon and Breach, New York, 1963), p. 125.

[16]T. Janssens, R. Hofstadter, E. B. Hughes, and M. R. Yearian, Phys. Rev. 142, 922 (1966).

[17]See, for example, J. W. Friar and J. W. Negele, in *Advances in Nuclear Physics*, edited by M. Baranger and E. Vogt (Plenum, New York, 1975), Vol. 8, Sec. 1.3.1.

[18]J. P. Jeukenne, A. Lejeune, and C. Mahaux, in *Lecture Notes in Physics, No. 55,* edited by S. Boffi and G. Passatore (Springer, Berlin, 1976), p. 68; A. Lejeune, private communications.

[19]A. Nadagen, P. Schwandt, P. P. Singh, A. D. Backer, P. T. Debevec, W. W. Jacobs, M. D. Kaitchuk, and J. T. Meek, Indiana report, 1979.

[20]J. P. Jeukenne, A. Lejeune, and C. Mahaux, Phys. Rep. C25, 83 (1976); J. P. Jeukenne, A. Lejeune, and C. Mahaux, Phys. Rev. C 16, 80 (1977).

[21]A. L. Fetter and J. D. Walecka, *Quantum-Theory of Many-Particle Systems* (McGraw-Hill, New York, 1971), p. 191.

[22]S.-O. Bäckman, A. D. Jackson, and J. Speth, Phys. Lett. 56B, 209 (1975).

[23]J. D. Vergados and H. W. Baer, Phys. Lett. 41B, 560 (1972).

[24]P. Singer, N. C. Mukhopadhyay, and R. D. Amado, Phys. Rev. Lett. 42, 162 (1979).

[25]W. Maguire and C. Werntz, Nucl. Phys. A205, 211 (1975).

[26]J. D. Vergados, Phys. Rev. C 12, 78 (1975).

[27]J. Mougey, M. Bernheim, D. Royer, D. Tarnowski, S. Turck, P. D. Zimmermann, J. M. Finn, S. Frullani, D. B. Isabelle, G. P. Capitani, E. De Sanctis, and I. Sick, Phys. Rev. Lett. 41, 1645 (1978); I. Sick, private communications.